The recoil correction to the proton-finite-size contribution to the Lamb shift in muonic hydrogen

Savely G. Karshenboim*
Max-Planck-Institut für Quantenoptik, Garching, 85748, Germany and Pulkovo Observatory, St.Petersburg, 196140, Russia

Evgeny Yu. Korzinin and Valery A. Shelyuto
D. I. Mendeleev Institute for Metrology, St.Petersburg, 190005, Russia

Vladimir G. Ivanov
Pulkovo Observatory, St.Petersburg, 196140, Russia

arXiv:1501.06539v1 [hep-ph] 26 Jan 2015

The Lamb shift in muonic hydrogen was measured some time ago to a high accuracy. The theoretical prediction of this value is very sensitive to the proton-finite-size effects. The proton radius extracted from muonic hydrogen is in contradiction with the results extracted from elastic electron-proton scattering. That creates a certain problem for the interpretation of the results from the muonic hydrogen Lamb shift. For the latter we need also to take into account the two-photon-exchange contribution with the proton finite size involved. The only way to describe it relies on the data from the scattering, which may produce an internal inconsistency of theory.

Recently the leading proton-finite-size contribution to the two-photon exchange was found within the external field approximation. The recoil part of the two-photon-exchange has not been considered. Here we revisit calculation of the external-field part and take the recoil correction to the finite-size effects into account.

PACS numbers: 12.20.-m, 13.40.Gp, 31.30.J-, 36.10.Ee,

I. INTRODUCTION

A few years ago the Lamb shift $(2p_{1/2} - 2s_{1/2})$ in muonic hydrogen was experimentally determined to a great accuracy [1]. The related theoretical prediction is much less accurate, suffering from a bad knowledge of the proton charge radius. Therefore, the experimental data and theoretical expression have been utilized to determine an accurate value of the proton radius. Actually, theory (see, e.g., [1–3]) disagrees with experiment and therefore the muonic-hydrogen value of the proton charge radius is inconsistent with results of hydrogen spectroscopy [4] and evaluations of the elastic electron-proton scattering (see, e.g., [5–8]).

The theoretical prediction for the Lamb shift in muonic hydrogen is basically of the form

$$\Delta E_L = c_1 + c_2\, R_E^2 \,, \qquad (1)$$

where the first term, dominated by the Uehling correction and other QED effects, does not depend on the proton rms electric charge radius R_E, and the second term is dominated by the leading proton-finite-size correction. Meanwhile, there is a higher-order proton-finite-size correction, which does depend on the distribution of the proton charge (or rather we prefer to discuss the electric charge form factor of the proton $G_E(q^2)$), but does not have the required form of $const \times R_E^2$.

The general problem in its calculation is that to find it one has to use a certain description of the charge distribution (or $G_E(q^2)$). There is no satisfactory *ab initio* model. So, one either could apply a certain variety of models, which are not really related to experimental data and arbitrary to a certain extent, and to estimate somehow the uncertainty, or, alternatively, one could take advantage of the existing experimental data. The first option does not really work for the proton. As for the second option, the experimental data by themselves are not accurate enough and one cannot use the data directly, Instead one has to apply a fit. Unfortunately, and that is a real problem with the proton radius, the fits also produce their value of R_E and those values from empiric fits do not agree with the value from the muonic hydrogen (see, e.g., parameters of low momentum expansion of some empiric fits in Table I).

We have to clarify that the correction we discuss here is a small one, while the contradiction is huge. The very fact and the scale of the discrepancy does not depend on the way we treat the higher-order proton-finite-size term. Meanwhile, the eventual value of the muonic R_E does depend on the way, we treat the higher-order finite-size correction, at the level of the uncertainty of R_E. Here we revisit the correction.

The higher-order proton-finite-size correction can be understood as a certain moment of the charge distribution. Since the very mean radius of that distribution is under question because the results from the scattering and the muonic hydrogen are different, we cannot directly apply the scattering results for these corrections (see, e.g., [9–12]).

*Electronic address: savely.karshenboim@mpq.mpg.de

Thus, the next-to-leading proton-finite size corrections are sensitive to detail of the charge distribution. A self-consistent consideration of those shape-sensitive contributions was performed in [12]. The consideration was done within the external field approximation, which delivers the leading part of the shape-sensitive contributions. Here, we present a complete evaluation, including recoil effects. Those involve not only the charge distribution, but also a distribution of the magnetic moment.

There are two main ingredients of our consideration. We have to explain the method of a treatment of the higher-order finite-size correction within a theory of muonic hydrogen, which would be consistent both with the experimental data on the electron-proton scattering and with the muonic value of the proton radius. The method has been applied previously [12] within the external field approximation. Here we are to expand it to accommodate the recoil finite-size corrections, which we also need to consider. For that we follow [13, 14]. In both cases we start following cited papers, but modify the approaches.

II. GENERAL EXPRESSION FOR THE ELASTIC TWO-PHOTON-EXCHANGE CONTRIBUTION

Let's start with the expression for the proton-finite-size contribution including the recoil effects. They are described by the two-photon exchange (TPE). The leading part of the higher-order proton-finite-size term is the so-called Friar term. That is a result derived within the external field approximation (see Fig. 1). The result for the correction was first derived in the coordinate space [15–17] and next in the momentum space [18] (see [2] for details of the derivation)

$$\Delta E_{\rm Fr}(nl) = -\frac{16(Z\alpha)^5\, m_r^4}{\pi}\, I_{\rm Fr}\frac{\delta_{l0}}{n^3}\,, \qquad (2)$$
$$I_{\rm Fr} = \int_0^\infty \frac{dq}{q^4}\left[\left(G_E(q^2)\right)^2 - 1 - 2G'_E(0)\, q^2\right]\,.$$

Here and throughout the paper we apply the relativistic units, in which $\hbar = c = 1$, m stands for the muon mass, M is the proton mass and m_r is the reduced mass. The momentum q is the Euclidean one.

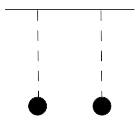


FIG. 1: The diagram for the Friar correction to Lamb shift in muonic hydrogen. The appropriate subtractions are assumed.

If we like to consider the TPE correction with all recoil effects included, we have to use a certain two-body formalism, such as the effective Dirac equation (EDE) [2, 19, 20]. Within such an approach the TPE diagrams appear with certain subtractions (related to proton pole contributions) and on top of those subtracted two-body TPE diagrams one has to add a perturbative series of an effective one-body theory, e.g., the EDE theory with a proton on mass shell. The latter is presented by the Friar contribution, while the former is related to two types of the effects. Those include elastic (with subtractions) and inelastic (polarizability) parts (see Figs. 2 and 3), which at a certain stage are to be considered together.

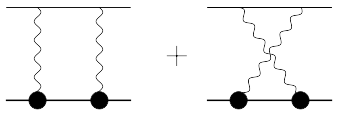


FIG. 2: Two-photon-exchange: elastic contribution. Necessary subtractions, which follow from an EDE consideration, are assumed. The circles are for the vertex with the appropriate form factors.

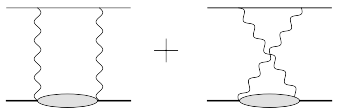


FIG. 3: Two-photon-exchange: inelastic contribution (the proton polarizability).

Indeed, once we have well-defined elastic and inelastic quantities, we can work on their calculation independently. However, their definition is not a straightforward issue. As an example one can consider a calculation of the elastic part. It requires an appropriate on-shell vertex for the proton. One may deal with the Dirac and Pauli form factors $F_{1,2}$ or with the Sachs ones $G_{E,M}$. The difference between those two parametrizations leads to a contribution, which vanishes for the on-shell vertex, but is not equal to zero for the TPE diagrams in Fig. 2, which involve the vertexes off-shell. In other words, the elastic part is not well-defined by itself.

Meanwhile, both elastic and inelastic contributions have their specifics and their calculation is very different. Indeed, there are distinguished contributions into each of them and those contributions can be studied independently of the definitions. One of them is the Friar term, the dominant part of the elastic TPE and we indeed can study it independently of anything else. (As we mention, the ambiguity in a possible definition of the elastic term concerns usually only recoil effects, while the Friar term is the result within the external field approximation.) Indeed, the actual expression for the elastic part for the two-photon-exchange (eTPE) correction is more complicated than the Friar contribution (2). Once we intend to complete the calculation of the elastic part and to add recoil corrections to the Friar term, we have to check the definitions.

Therefore, we have to explicitly quote the definitions of the elastic and inelastic TPE and to be sure they are consistent. While calculations of the elastic and inelastic parts of TPE have been done in a single paper for a few occasions [21–23], the first complete evaluation of TPE, where consistency of their definitions was discussed, appeared some time later in [13]. Unfortunately, it did not manage to produce consistent definitions of the elastic and inelastic part. The consistency was achieved later in [14].

The elastic part of the TPE contribution consists of a QED result for a point-like proton and of a proton-structure correction. We acknowledge that the point-like part has been already calculated and it is subtracted while calculating the eTPE term. The QED TPE term is the well-known Salpeter contribution (see, e.g., [2, 20]). It is for the proton without any anomalous magnetic moment, which satisfies the conditions $F_1(0)=1, F_2(0)=0$ or $G_E(0)=G_M(0)=1$.

The analytic expression for the eTPE contribution was considered in [13, 14, 21, 22]. Here, we re-arrange the expression for our purpose. The general structure is of the form [13, 14] (cf. [21, 22])

$$\begin{aligned}
\Delta E_{\rm eTPE}(nl) &= -\frac{16(Z\alpha)^5\,m_r^4}{\pi}\,I_{\rm eTPE}\frac{\delta_{l0}}{n^3}\,,\\
I_{\rm eTPE} &= I_{\rm Fr}+I_{\rm rec}\,,\\
I_{\rm Fr} &= \int_0^\infty\frac{dq}{q^4}\left[\bigl(G_E(q^2)\bigr)^2-1-2G'_E(0)\,q^2\right]\,,\\
I_{\rm rec} &= I_{\rm E}+I_{\rm M}+I_{\rm F}\,,\\
I_{\rm E} &= \int_0^\infty\frac{dq}{q^4}f_E(m,M;q^2)\left[\bigl(G_E(q^2)\bigr)^2-1\right]\,,\\
I_{\rm M} &= \int_0^\infty\frac{dq}{q^4}f_M(m,M;q^2)\left[\bigl(G_M(q^2)\bigr)^2-1\right]\,,\\
I_{\rm F} &= \int_0^\infty\frac{dq}{q^4}f_F(m,M;q^2)\left[\bigl(F_1(q^2)\bigr)^2-1\right] \qquad (3)
\end{aligned}$$

The Dirac form factor

$$F_1(q^2)=\frac{G_E(q^2)+\frac{q^2}{4m_p^2}\,G_M(q^2)}{1+\frac{q^2}{4m_p^2}}$$

is more fundamental than the Sachs electric and magnetic form factors G_E and G_M. However, just the latter are used to be fitted in empiric-fit papers.

The last term, $I_{\rm F}$, was excluded in [13] from the elastic part and attributed to the polarizability. Later on, it was re-established by [14] as a part of the elastic TPE. Most of the existing results on the polarizability [14, 21, 23–26] are consistent with this definition[1] or, as in case of [27], can be re-adjusted to it.

[1] Actually, the very calculation of the polarizability in [13] is consistent with the definition of the elastic part including this term as was shown in [14].

The first term apparently is the Friar term, which is a non-recoil contribution. The other terms are for the recoil. As it happens in the two-body systems (see, e.g., various corrections to the Lamb shift in [2]) the external-field contributions and the recoil one are treated differently and they have different subtractions. The structure G^2-1 is a result of the subtraction of the expression for the point-like proton.

The explicit presentation of the f factors [13] is

$$\begin{aligned}
f_E(m,M;q^2) &= \frac{q}{2(M-m)}\left[\left(\frac{\gamma_2(\tau_p)}{\sqrt{\tau_p}}-\frac{\gamma_2(\tau_\mu)}{\sqrt{\tau_\mu}}\right)\frac{1}{1+\tau_p}\right.\\
&\quad\left.-\left(\frac{1}{\sqrt{\tau_p}}-\frac{1}{\sqrt{\tau_\mu}}\right)\right]\,,\\
f_M(m,M;q^2) &= \frac{q\,\tau_p}{2(M-m)}\left[\left(\frac{\gamma_2(\tau_p)}{\sqrt{\tau_p}}-\frac{\gamma_2(\tau_\mu)}{\sqrt{\tau_\mu}}\right)\frac{1}{1+\tau_p}\right.\\
&\quad\left.-\left(\frac{\gamma_1(\tau_p)}{\sqrt{\tau_p}}-\frac{\gamma_1(\tau_\mu)}{\sqrt{\tau_\mu}}\right)\right]\,,\\
f_F(m,M;q^2) &= \frac{M+m}{m}\,\tau_p\gamma_1(\tau_\mu)\,, \qquad (4)
\end{aligned}$$

where

$$\begin{aligned}
\tau_p &= \frac{q^2}{4M^2}\,,\\
\tau_\mu &= \frac{q^2}{4m^2}\,,\\
\gamma_1(\tau) &= (1-2\tau)\left(\sqrt{1+\tau}-\sqrt{\tau}\right)+\sqrt{\tau}\,,\\
\gamma_2(\tau) &= (1+\tau)^{3/2}-\tau^{3/2}-\frac{3}{2}\sqrt{\tau}\,. \qquad (5)
\end{aligned}$$

We are going to treat electric and magnetic form factors somewhat different and we are to decompose the Dirac form factor

$$\begin{aligned}
F_1^2-1 &= \frac{1}{(1+\tau_p)^2}(G_E^2-1)+\frac{2\tau_p}{(1+\tau_p)^2}(G_MG_E-1)\\
&\quad+\frac{\tau_p^2}{(1+\tau_p)^2}(G_M^2-1) \qquad (6)
\end{aligned}$$

into terms of the Sachs form factors. We also note that the eTPE contribution takes into account two structure effects, which are a non-zero value of the anomalous magnetic moment of the proton $F_2(0)=G_M(0)-1=\kappa\simeq 1.792\,85$ and the finite size of the proton. It is helpful to disentangle them because the former can be found with a very high accuracy, while the latter as we will show (see also [12]) needs for its calculation additional experimental data and is not free from uncertainties.

Eventually, we arrive at

$$
\begin{aligned}
I_{\rm rec} &= I_\kappa + I_{\rm EF} + I_{\rm M1} + I_{\rm M2} \\
I_\kappa &= \kappa \int_0^\infty \frac{dq}{q^4} \left\{ (2+\kappa) f_{M1} + f_{M2} \right\} , \\
I_{\rm EF} &= \int_0^\infty \frac{dq}{q^4} f_{EF}(m, M; q^2) \left[\left(G_E(q^2) \right)^2 - 1 \right] , \\
I_{\rm M1} &= \int_0^\infty \frac{dq}{q^4} f_{M1} \left[\left(G_M(q^2) \right)^2 - (1+\kappa)^2 \right] , \\
I_{\rm M2} &= \int_0^\infty \frac{dq}{q^4} f_{M2} \left[G_M(q^2) G_E(q^2) - (1+\kappa) \right] , \quad (7)
\end{aligned}
$$

where

$$
\begin{aligned}
f_{\rm EF} &= f_E + \frac{1}{(1+\tau_p)^2} f_F , \\
f_{\rm M1} &= f_M + \frac{\tau_p^2}{(1+\tau_p)^2} f_F , \\
f_{\rm M2} &= \frac{2\tau_p}{(1+\tau_p)^2} f_F . \quad (8)
\end{aligned}
$$

We can compare the integrands related to various contributions to $I_{\rm eTPE}$ as summarized in Fig. 4. The plot is prepared using the standard dipole approximation

$$
G_{\rm dip}(q^2) = \left(\frac{\Lambda^2}{q^2 + \Lambda^2} \right)^2 \quad (9)
$$

(with $\Lambda^2 = 0.71\,{\rm GeV}^2$), which is good to estimate the size of various contributions, but is not accurate enough for real calculations.

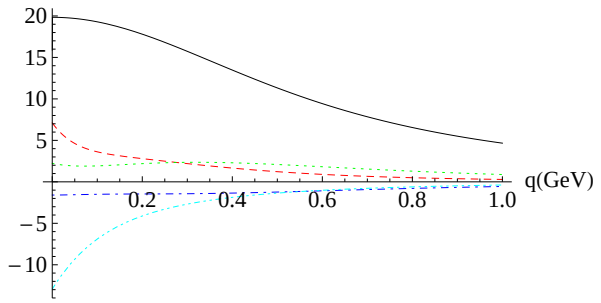


FIG. 4: Integrands for the individual contributions to $I_{\rm eTPE}$: for the Friar term (2) (the black line), the κ term (the cyan dot-dot-dashed line), the EF term (the red dashed line), the $M1$ term (the green dotted line), and the $M2$ term (blue dot-dashed line).

III. A PRELIMINARY CONSIDERATION

As we see from the plot, the Friar term is indeed the dominant contribution. However, that is not only the value of the contribution that matters. The uncertainty is not necessary related to the size of the contribution. The Friar term is not only the dominant term for the eTPE contribution, but it is also the part of eTPE, which is the most sensitive to the parametrization of the form factors. The sensitivity of this term to the parametrization was discussed in [12].

The situation with accuracy of the data for the integration is presented in Fig. 5 taken from [12]. The estimations are made within the dipole parametrization.

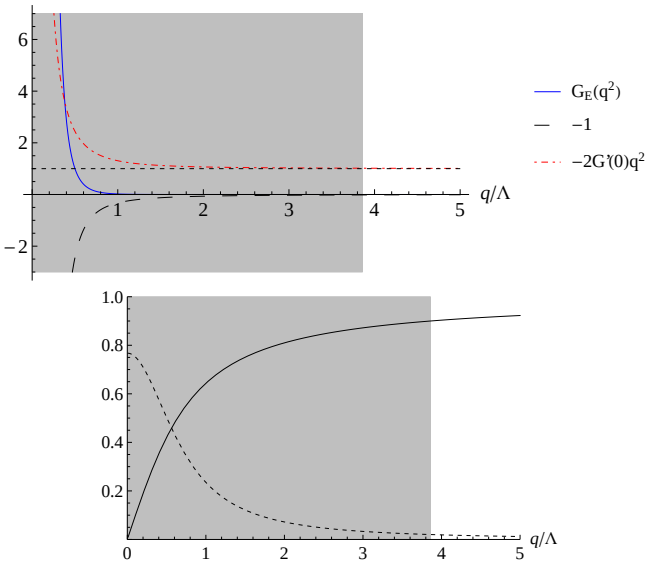


FIG. 5: Top: Fractional contributions to the integrand of $I_{\rm Fr}$ in (2) as a function of q/Λ as follows from the dipole model. The red dot-dashed line is for the subtraction term with $G'(0)$. The dashed line is for the subtraction term with 1 and the blue solid line is for the G^2 term, which represents the data. Bottom: the integrand (in arbitrary units) is presented with a dashed line and the integral $\int_0^q dq/q^4 \left[(G_E(q^2))^2 - 1 - 2G'_E(0)\, q^2 \right]$ (in fractional units) in presented as a function of q with a solid line. The shadow belt is for the area in the q space from which 90% of the integral $I_{\rm Fr}$ come. See [12] for detail.

The gray area is for the area, where 90% of the integral comes from. One sees that below $0.6\Lambda \simeq 0.5$ GeV there is a massive cancellation between the data term (with $G_E(q^2)$) and the subtractions terms (with 1 and with $G'(0)$). The data on $G_E(q^2)$ roughly have accuracy at the 1% level and below this point the accuracy of the integrand becomes worse than 1% and increases very fast. Meanwhile, above $0.8\Lambda \simeq 0.65$ GeV, the contribution of the data themselves (i.e. of the $G_E(q^2)$ term) is negligible, while the subtraction term with $G'_E(0)$ dominates.

Therefore, the integrand at low momentum is determined by our knowledge of the curvature of $(G_E(q^2))^2$, while at high momentum it is determined by the slope of $(G_E(q^2))^2$. Both values cannot be measured experimentally, but can be extracted on base of a certain fitting procedure. Except for the κ term, the integrand of which

does not involve the data on the form factors, the other data are also sensitive to the fittings. At low momentum all the integrands are determined by the slope of the related G^2 terms and thus are proportional to the electric and/or magnetic radius squared. Indeed, any fitting produces a certain systematic uncertainty.

Unfortunately, the determination of neither electric nor magnetic radius is free of questions. Different extractions from different kinds of data lead to inconsistent results. We have already mentioned a strong discrepancy between muonic-hydrogen R_E [1] and the scattering values (see, e.g., [5–8]). The results on R_M are not in a perfect shape as well (see, e.g., [11, 28]). However, the discrepancy in determination of R_M from MAMI [5] and global data [6] is not that important. The most important is that the determination of the charge radius R_E from the scattering and muonic hydrogen is not in agreement, which compromises the whole procedure. Meanwhile, the magnetic radius is even more sensitive to various systematic effects [29–31].

As we mentioned, we discuss a rather small correction. We anticipate that a different treatment of the higher-order proton-size contribution will somewhat shift the value of R_E from muonic hydrogen, but not significantly (cf. [12]). So, we expect that the discrepancy will remain and we have to find a way how to use the scattering data without a contradiction to the finally extracted value.

We intend to use fits, rather than the data. Generally speaking, to find an appropriate fit is a tricky issue. A pure empiric fit is the best suited to fit the data, however, it ignores various theoretical constraints and constraints which follow from some other scattering channels (through theory). On the contrary, a fit, which follows all those constraint, either may disagree with the data or may involve so complicated fit function that it would produce instabilities. Therefore, we prefer to use empiric fits, but we intend to apply them in a specific way.

There are two ways to apply empiric fits. E.g., when one evaluates the hadronic vacuum polarization contribution to the anomalous magnetic moment of muon (see, e.g., [32]), there is no subtraction involved. The fit is necessary only as a smooth approximating curve which is consistent with all the data involved. Its parameters by themselves are irrelevant. The other story is when the parameters of the fit are really applied. In the integral in (2) they are. The very shape of an empiric fit has no physical sense. The parameters must be applied with a caution. A scenario, in which the result for the Friar correction does not depend on the low-q^2 behavior of the fit, was developed in [12].

The most plausible scenario to explain the discrepancy between the scattering and muonic-hydrogen values of R_E is that the scattering data are more or less correct, but the accuracy in determination of the radius is overestimated. The alternatives, such as a suggestion that the data are not correct or the muonic value is wrong, are not an option here. If the muonic value is wrong, there is no sense in a calculation of small corrections while the discrepancy is that large. The scattering data from different experiments are consistent and it is hard to imagine that they are completely wrong.

The integrand involves massive cancellations at low q domain, while for high q it is dominated by the contribution, proportional to

$$G'_E(0) = -\frac{1}{6} R_E^2 \,. \tag{10}$$

If one calculates the integral using scattering data, as it was done, e.g., in [13], the value of $G'_E(0)$ is indeed taken from there and it is inconsistent with R_E from the Lamb-shift. If one calculated the whole integral as a single thing, then there is no other choice because if we take a value of $G'_E(0)$ inconsistent with the applied fit for $G_E(q^2)$, the integral is infrared divergent.

Following [12], our treatment of the Friar term is based on two important steps. First, following [9, 12], we split the integration into two parts

$$I = \int_0^\infty dq ... \equiv I_< + I_> \equiv \int_0^{q_0} dq ... + \int_{q_0}^\infty dq ... \,. \tag{11}$$

Those two terms are to be treated differently.

The separation disentangles the subtraction at low q and the asymptotic behavior at high q, which both involve $G'_E(0)$, and, in particular, that allows to use for the high-q asymptotics the physical value of R_E. This value is not fixed, being an adjustable parameter to be eventually found from a comparison of the theory and experiment on the muonic-hydrogen Lamb shift. In this area we integrate the G^2 term and the subtractions separately and while integrating G^2 we rely on the empiric fits.

Meanwhile, at the low-q part of the integral we rely on the expansion of the form factor

$$\big(G_E(q^2)\big)^2 \simeq 1 - \frac{R_E^2}{3} q^2 + K\, q^4 \,. \tag{12}$$

Even a very bold estimation of the K coefficient allows at low q a better accuracy than the data by themselves (see [12] and consideration below).

The final result takes the form

$$I = C_{R_E^2}\, R_E^2 + \widehat{I} \,. \tag{13}$$

Such a form of presentation is crucial, allowing a self-consistent consideration. As the result, the theoretical expression for the Lamb shift in muonic hydrogen keeps the desirable form as in (1) and the higher-order proton-finite-size term (2) contributes to both coefficients c_1 and c_2. Meantime, we use the empiric fits only in the area of the high-q part of the integrand and the result only marginally depends on the details of their extrapolation to $q^2 = 0$ (see [12] and consideration below). As a final important step, we have a free parameter q_0 which we are to vary to minimize the uncertainty of the calculations.

IV. CALCULATION OF THE LEADING PROTON-FINITE-SIZE TPE CONTRIBUTION (THE FRIAR TERM)

Let's consider evaluation of the leading proton-finite-size TPE contribution $I_{\rm Fr}$ in more details. To deal with a lower-momentum contribution

$$I_{\rm Fr<} = \int_0^{q_0} \frac{dq}{q^4} \left[\left(G_E(q^2)\right)^2 - 1 - 2G'_E(0)\, q^2 \right]$$

we expand the form factor

$$\left(G_E(q^2)\right)^2 \simeq 1 - \frac{R_E^2}{3} q^2 + K^{\rm dip}(1 \pm 1)\, q^4 \,, \qquad (14)$$

and, following [12], we estimate the q^4 coefficient with help of the standard dipole model ($K^{\rm dip} = 10/\Lambda^4 \simeq 19.8$ GeV^{-4}). The dipole formula is not that bad for bold estimations. E.g., the $G'(0)$ terms are different from the value following from the muonic R_E by roughly 7% and from those following from hydrogen-and-deuterium spectroscopy's R_E and from scattering's R_E by about 17%. The uncertainty of 100% for the curvature seems reasonable. The value is also consistent with the curvature of various empiric fits (see, e.g., [33–38]; see also a discussion below).

The physical condition on the expansion is $q_0 < 2m_\pi \simeq 0.28$ GeV. We are to vary q_0 to minimize the final uncertainty and we will check this constraint after we specify the optimal value of q_0.

The expansion (14) allows to easily find the low-momentum contribution and its uncertainty

$$I_{\rm Fr>} = 10\,(1 \pm 1)\,\frac{q_0}{\Lambda^4} \,. \qquad (15)$$

For the low-q part we have exactly followed [12], while for the high-momentum part we prefer a certain alternation, which would be more suitable for the calculation of the recoil corrections. The higher-momentum part contains the data-related and radius-related contributions

$$I_{\rm Fr>} = \int_{q_0}^{\infty} \frac{dq}{q^4} \left(G_E(q^2)\right)^2 - \frac{1}{3q_0^3} + \frac{1}{3}\frac{R_E^2}{q_0} \,. \qquad (16)$$

Combining the low-q^2 and high-q^2 contributions, we find

$$\begin{aligned} \widehat{I}_{\rm Fr} \;&=\; \int_0^{q_0} \frac{dq}{q^4} \left[\left(G_E(q^2)\right)^2 - 1 - 2G'_E(0)\, q^2 \right] \\ &\quad + \int_{q_0}^{\infty} \frac{dq}{q^4} \left[\left(G_E(q^2)\right)^2 - 1 \right] \,, \\ C_{R_E^2:{\rm Fr}} \;&=\; \frac{1}{3q_0} \,, \end{aligned} \qquad (17)$$

which is necessary for the decomposition according to (13).

To calculate the central value of the data-related term in (16), the integration in [12] was done over the fits [33–37] (see Appendix A) and as the result the related median value was taken. Here, we use the most recent empiric fit from [37]

$$G_E(q^2) = \frac{1 + 2.909\,66\tau_p - 1.115\,422\,29\tau_p^2 + 3.866\,171\times10^{-2}\tau_p^3}{1 + 14.518\,7212\tau_p + 40.883\,33\tau_p^2 + 99.999\,998\tau_p^3 + 4.579\times10^{-5}\tau_p^4 + 10.358\,0447\tau_p^5} \,, \qquad (18)$$

where τ_p is defined above in (5). We estimate our knowledge of the form factors as at the level of 1% and expect that the dominant contribution to the integral for G^2 comes from a relatively small area around the low limit (cf. [12]). So, we expect the whole G^2 contributions known at the level of 2% and thus we arrive at

$$I_{\rm Fr>} = \int_{q_0}^{\infty} \frac{dq}{q^4} \left(G_E(q^2)\right)^2 \times \left(1 \pm 0.02\right) - \frac{1}{3q_0^3} + \frac{1}{3}\frac{R_E^2}{q_0} \,, \qquad (19)$$

where $G_E(q^2)$ is taken from (18).

While choosing the fits, we have looked for those which produce a smooth function for the all space-like q^2 and have a good value of the reduced χ^2. We prefer 'simple' empiric fits. We believe that it is tricky to determine the accuracy for the extrapolation to low q^2 and for the subsequent differentiation (to find R_E) and, most probably, their inconsistency with the muonic value of the proton radius is due to an overestimation of their accuracy. Nevertheless, the form factor by itself (not its derivative) is fitted by those fits well. The accuracy of the application of the fits was estimated in [12] separately as

$$\delta I_{\rm Fr>} = \frac{1}{3q_0^3} \frac{2\delta G_E(q_0^2)}{G_E(q_0^2)} \left(G_{\rm dip}(q_0^2)\right)^2 \,, \qquad (20)$$

where we expect that $\delta G_E(q_0^2)/G_E(q_0^2) \simeq 1\%$.

Here, we apply a somewhat different estimation of the uncertainty. It is estimated as 2% of the G^2 contribution into $I_{\rm Fr>}$. The dominant part of the G^2 integral comes from the low end of the integration area and as far as the low-end area dominates the estimations are close.

Above we explained that it is not consistent to use any fits. However, we need to distinguish using of the central value of the fits with a pre-estimated uncertainty, as we do, and the use of the parameters of the fits to find, e.g.,

some derivatives etc. If the fit over a large sample of the data has the reduced χ^2 about unity, that means that the fit is consistent with the data at the level of their uncertainty, which is about 1%. Such use of the fit does not assume any model. Once one intends to take advantages of the large number of data points and to obtain a certain value, e.g., $G'(0)$ with a high precision because of statistical average, the model comes out and the systematic uncertainty due to its application is to be estimated. We prefer to stay on the safe side and introduce the uncertainty at the level of the accuracy of the data which grants model independence while applying any fit with a good χ^2 value.

The scatter due to choice of the parametrization (i.e. due to choice of the fits [33–37]) is smaller than the uncertainty we introduced. The reason for the bigger value of the uncertainty is that all the fits basically fitted the same data, which were only partly updated from a publication to a publication. The scatter does not reflect the accuracy of the data, but rather the importance of their updates. The uncertainties of $I_{\rm Fr<}$ and $I_{\rm Fr>}$ are considered as independent.

Fit	Ref.	Type	R_E [fm]	K [GeV^{-4}]
(A1)	[34]	chain fraction	0.90	34.3
(A3)	[34]	chain fraction	0.90	35.3
(A5)	[33]	Padé approximation (q^2)	0.86	28.0
(A7)	[35]	Padé approximation (q^2)	0.88	31.1
(A9)	[36]	Padé approximation (q^2)	0.87	28.2
(18)	[37]	Padé approximation (q^2)	0.88	31.3

TABLE I: The low-momentum expansion of the fits for the electric form factor of the proton applied in [12]. The values are given for central values of the fits without any uncertainty. Here: $\left(G_E(q^2)\right)^2 = 1 - R_E^2 q^2/3 + Kq^4 + ...$ The related values for the standard dipole fit are $R_E = 0.811$ fm and $K = 19.8$ GeV^{-4}. The spread of the central values of the charge radius (from 0.86 to 0.90 fm) for different fits (from different sets of the data) is comparable with the spread of central values of the updated results on the proton radius, obtained by different methods, the central values of which are 0.84 fm (μH [1]), 0.88 fm (H&D [4]), 0.895 fm (global data without MAMI [6]—and the results of the other evaluations are similar) and 0.88 fm (MAMI [5]). All the values, but from muonic hydrogen, have uncertainty at the level of 1%. The muonic one is much more accurate.

To facilitate further numerical evaluations with including the recoil effects, we choose here instead of the median the fit [37], which is the most recent one. This modification is not important because our estimation of the uncertainty is substantially larger than the scatter. The most of the integral (for the G^2 term) comes from the low limit. Here, we choose to assign the 2% uncertainty to the whole G^2 term. We have checked that this modification is of marginal importance for the Friar term, however, as we mentioned, it simplifies a comparison with [13]. Note, that is not an improvement, but a simplification. The reason to check the median using various fits (some of which are partly out of date) was to check that the result does not much depend on low-q^2 behavior. The spread of the values of the radius was sufficient to prove such model independence, which was also confirmed by the use a fit from [39], which, despite of unreasonable low-q behavior, produces a quite reasonable result. Only after such tests are performed, the use of the most recent fit is possible.

The extracted value of the proton radius depends on the separation parameter q_0 in almost the same way as for [12]. The procedure (see [12] and sections below) allows to vary the value of the separation parameter q_0 and to find an optimal one. The results with different values of q_0 are consistent. The deviation from the former treatment of the eTPE [13] is large enough (at the level of the uncertainty) to be considered seriously. The dependence $R_E(q_0)$ is shown in Fig. 6.

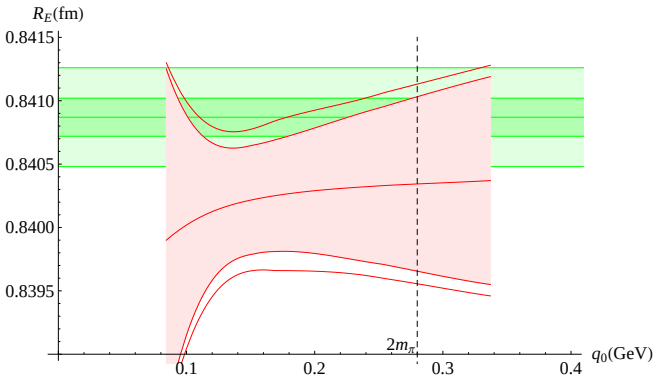


FIG. 6: The value of the proton charge radius R_E extracted [12] from measurement [1] of the muonic-hydrogen Lamb shift. The plot follows [12]. The horizontal belt is for the original value of the parameter. The other figure [of a more complicated shape] is for the radius determined in [12], presented as a function of the separation parameter q_0. Every area corresponds to one sigma. The internal and darker part of each figure is related to the partial uncertainty due to the calculation $I_{\rm Fr}$, while the whole area is for the total uncertainty of the radius. The final result of [12] $R_E = 0.840\,22(56)$ fm was obtained there at the optimal value $q_0 \simeq 0.152$ GeV.

Minimizing the uncertainty we arrive at

$$I_{\rm Fr} = \frac{1}{3}\frac{R_E^2}{q_0} - 23.5(3.3)\ \text{GeV}^{-3}\,, \qquad (21)$$

where the numerical value corresponds to $q_0 \simeq 0.147$ GeV. It is important that the new optimal value is quite below $2m_\pi$ which is the requirement for the validity of the expansion (14).

While the decomposition R^2 term and into the con-

stant $\widehat{I}$ is somewhat different[2], the related numerical results at $R_E = 0.84$ fm are in a perfect agreement, being 17.6(3.4) GeV^{-3} [12] and 17.7(3.3) GeV^{-3} (this work). The approach applied here is a modification of the one from [12] and the results for the radius are expected to nearly coincide at $R_E = 0.84$ fm. The latter effectively means that the extracted radius is to be approximately the same (with a marginal deviation). (We widely use in this paper the 'reference' value of various contributions at $R_E = 0.84$ fm—that is the approximate value consistent with extractions from the muonic hydrogen [1, 12] at the level of 10^{-3} which is completely sufficient taking into account the uncertainty of our calculations of the Friar and eTPE integrals at the level of 20%.)

Those numerical values should be compared with the results which can be obtained if one directly applies empiric fits to (2). The related results are $I_{\rm Fr} = 23.1(1.1)$ GeV^{-3} (after applying empiric fits [40]), 22.9(1.2) GeV^{-3} (after applying [12] empiric fits [35] and [33] — that is similarly to consideration in [13], which was done for the complete $I_{\rm eTPE}$) and $I_{\rm Fr} = 24.3(7)$ GeV^{-3} (after applying empiric fits [10]). The uncertainty of our result is essentially larger than theirs and the the shift from the quoted values to ours is larger than the uncertainty. We believe that the uncertainty of the cited results was underestimated and suffered from an inconsistency (once we accept the muonic value for the proton radius).

We have to recall the geometrical meaning of the Friar term

$$I_{\rm Fr} = \frac{\pi}{48}\int d^3r \int d^3r' |\mathbf{r}-\mathbf{r}'|^3 \rho(\mathbf{r})\rho(\mathbf{r}') \ , \qquad (22)$$

where in a non-relativistic approximation $\rho(\mathbf{r})$, being a Fourier transform of $G_E(\mathbf{q})$, is the charge density inside the proton. The muonic-hydrogen data assume a smaller proton, thus the Friar term adjusted to those data should also be smaller (see also discussion on that in [10]). The radius is smaller by about 6% than the results from the empiric fits and the Friar term (the central value) is smaller by about 15%, which seems consistent.

Indeed, in a rigorous consideration, the Fourier transform of G_E is not the charge density in common sense. However, the presence of relativistic effects does not affect the fact that the value of the Friar term is determined to a certain extent by the proton size, it just makes this relation more complicated and involves corrections. The non-relativistic part with a clear geometric sense remains and it is dominant.

One may wonder whether splitting the area of the integration maintains the continuity of the form factor. We cannot check it *a priori* because at low q^2 we use the actual value of the proton radius. However, once the complete calculation is performed, we find the value of the radius and can to check the continuity. Such an *a posteriori* test is plotted in Fig. 7. The red area is for the low-q^2 expansion and the green one is the fit from [37] suggesting the uncertainty of 1%. They are consistent.

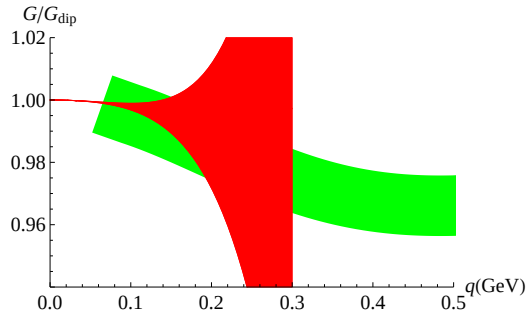


FIG. 7: The continuity test for the proton electric form factor normalized against the standard dipole fit. The red area on the left with fast increasing (to the right) width is for the low momentum approximation, while the belt with approximately homogenous width on the right is for the empiric fit [37] we used, with the uncertainty of 1%.

The method suggested in [12] pretends that the result does not depend on the parametrization of the fit. To check that, a number of fits have been applied (see Fig. 8). Those include the chain-fraction fits (in q^2) [35] (the blue dashed line), the Padé-approximation (in q^2) fits [33, 35, 36] (the green dot-dashed lines) and [37] (the green bold solid line), and a fit with the inverse polynomials in q [39] (the solid red line). The fits except for [39] have reasonable low q behavior. They are analytic in q^2 around $q^2 = 0$ and the related value of the charge radius varies from 0.86 to 0.90 fm, so the spread is comparable with the distance to the muonic value of 0.84 fm (see Table I). The high-q^2 asymptotics is proportional to q^{-2} for the chain fractions and to q^{-4} for the Padé approximations. Therefore, the parameters and the general behavior (far from the characteristic q_0 area) vary very much. Nevertheless, the spread of the values for the integral $I_{\rm Fr>}$ is smaller than the estimation of the uncertainty [12]. The scatter of the results with inclusion of the fit with unrealistic behavior [39] is somewhat larger than the uncertainty but still acceptable [12].

V. CALCULATION OF THE RECOIL CORRECTIONS

After discussing the leading eTPE term (within the external field approximation), we are prepared to consider the eTPE recoil corrections to it. We start from (7). As we see from Fig. 4, the dominant proton-finite-size terms are the EF and the κ ones. The former is the proton-size term, while the latter is not related to the proton size

[2] The result of [12] is $I_{\rm Fr} = R_E^2/(3q_0) - 22.2(3.4)$ GeV^{-3}, where the numerical value uses the optimal value $q_0 \simeq 0.152$ GeV. (Indeed, since the uncertainty of $I_>$ for the Friar term is defined here and in [12] differently, the optimal values, which minimize the uncertainty, are also somewhat different.)

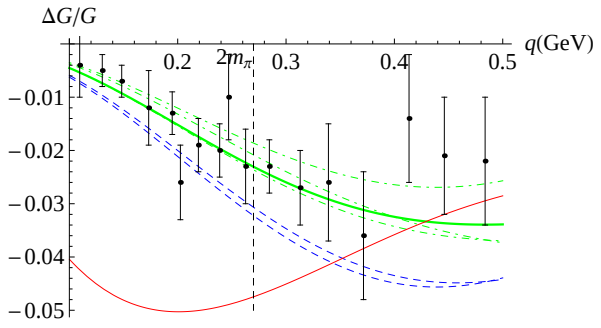


FIG. 8: The fractional deviation of the fits (see in App. A for details) and the data for the electric form factor $G_E(q^2)$ from the standard dipole form factor. The data are taken from [35], where the proton form factors were extracted from experimental data on the elastic electron-proton scattering. The fits include the chain-fraction fits (A1) and (A3) (in q^2) [35] (the blue dashed line), the Padé-approximation (in q^2) fits (A5), (A7), (A9), and (18) [33, 35, 36] (the green dot-dashed lines) with the most recent one from [37] shown with a green bold solid line. An exceptional fit (A12) with an inverse polynomials in q [39] is shown with a solid red line.

directly. Domination of the EF term is due to q/M expansion. Comparing the coefficient functions at the area of $m \ll q \ll M$ we find

$$\begin{aligned} f_{\rm EF}(m,M;q^2) &\simeq -\frac{3}{8}\frac{q}{M}\,, \\ f_{\rm M1}(m,M;q^2) &\simeq -\frac{3}{16}\left(\frac{q}{M}\right)^3\,, \\ f_{\rm M2}(m,M;q^2) &\simeq \frac{3}{16}\left(\frac{q}{M}\right)^3\,, \end{aligned} \tag{23}$$

which explains why the EF term is dominating.

An important area of the integration is related to $q \sim m$ and it is useful to present a more detailed asymptotics at $m \ll M$, $q \ll M$ (exactly in m/q)

$$f_{\rm EF} = -\frac{q^4\left(\sqrt{4m^2+q^2}-q\right)+8m^4\left(\sqrt{4m^2+q^2}-2m\right)-2m^2q^3}{16m^4M}+\dots \tag{24}$$

Decomposing the EF term according (13) we find

$$\begin{aligned} \widehat{I}_{\rm EF} &= \int_0^{q_0}\frac{dq}{q^4}\left[\left(G_E(q^2)\right)^2-1-2G_E'(0)\,q^2\right]f_{\rm EF}(q^2) \\ &\quad+\int_{q_0}^{\infty}\frac{dq}{q^4}\left[\left(G_E(q^2)\right)^2-1\right]f_{\rm EF}(q^2)\,, \\ C_{R_E^2:{\rm EF}} &= -\frac{1}{3}\int_0^{q_0}\frac{dq}{q^2}f_{\rm EF}(q^2)\,. \end{aligned} \tag{25}$$

That is very similar to the expression (17) for the Friar term. The evaluation of the integrals is done in a similar way and we apply the same effective description for G_E. The only difference is that in former case all the integrals except for the G^2 term were calculated analytically, while here we have to do that numerically.

The other important term is the κ term. It is a proton-structure correction, but not a proton-finite-size one. Since we decompose elastic TPE into the point-like Salpeter term and a proton-structure term, the subtraction in the latter is due to a proton without any anomalous magnetic moment. Therefore, there is a contribution to eTPE which does not vanish in the limit $R_E = R_M = 0$, which is the κ term. It does not involve the parametrization of the form factors and may be found with a high accuracy. We obtained the result from both numerically

$$I_\kappa = -2.850\,23\ {\rm GeV}^{-3} \tag{26}$$

and in a close analytic form

$$\begin{aligned} I_\kappa &= \frac{\kappa}{16\,M^2(M-m)}\cdot\left[-3(1+\kappa)\ln\frac{M}{m}\right. \\ &\quad\left.+(1-\kappa)\left(\ln 2-\frac{1}{4}\right)+B\cdot\left(\frac{m}{M}\right)^2\right]\,. \end{aligned} \tag{27}$$

where the value of $B \sim \mathcal{O}(1)$. Our result for this value is

$$\begin{aligned} B &= \left[\frac{\kappa-2}{4}\ln\frac{2M}{m}+\frac{2+11\kappa}{48}\right] \\ &\quad+\left[\frac{\kappa-3}{16}\ln\frac{2M}{m}-\frac{43(1+\kappa)}{384}\right]\left(\frac{m}{M}\right)^2+\dots \end{aligned}$$

As one sees (cf. (23)), this term is $\sim M^{-3}$ in contrast to the leading part of the EF term, which is $\sim M^{-1}$. However, the non-vanishing value of κ, which enters the combinations such as $\kappa(1+\kappa)$, produces a certain enhancement.

Let's now consider the magnetic finite-size terms, $I_{\rm M1}$ and $I_{\rm M2}$. At low-q we use expansion

$$\left(G_M(q^2)\right)^2 = \mu_p^2\left(1-\frac{R_{\rm dip}^2}{3}q^2[1\pm 0.4]+K^{\rm dip}q^4(1\pm 1)\right)\,, \tag{28}$$

where $\mu_p = 1+\kappa_p \simeq 2.792\,85$ is the proton magnetic moment in the units of the nuclear magnetons, for the magnetic form factor, similar to that for the electric one. However, there is a difference. While for the electric form factor the value of R_E is the adjustable parameter for the

extraction of the charge radius from muonic hydrogen, the rms magnetic radius R_M should be a constraint. We use here the dipole value of the radius

$$R^2_{\rm dip} = \frac{12}{\Lambda^2} \,,$$

but with a conservative uncertainty of 40% (to R^2_M).

As for the high-q, we apply the fits from [37], which gives not only the fit for the electric form factor (18), but also a fit for the magnetic one. The latter is of the form

$$\frac{G_M(q^2)}{\mu_p} = \frac{1 - 1.435\,73\tau_p + 1.190\,520\,66\tau_p^2 + 0.254\,558\,41\tau_p^3}{1 + 9.707\,036\,81\tau_p + 3.7357\times 10^{-4}\tau_p^2 + 6.0\times 10^{-8}\tau_p^3 + 9.952\,7277\tau_p^4 + 12.797\,7739\tau_p^5} \,. \tag{29}$$

q_0 [GeV]	$C_{R_E^2}$ [GeV^{-1}]	$\widehat{I}_{\rm eTPE}$ [GeV^{-3}]	$I_{\rm eTPE}$ [GeV^{-3}]
0.1	3.362 20	−44.52	16.4(6.0)
0.2	1.714 65	−12.79	18.3(4.0)
0.3	1.175 25	−2.597	18.7(5.8)
0.4	0.911 53	2.527	19.1(7.6)
0.5	0.757 09	5.790	19.5(9.2)

TABLE II: The results $\widehat{I}$ and $I_{\rm eTPE}$ for fits (18) and (29) at various q_0. The last column is for the numerical value of $I_{\rm eTPE}$ at $R_E = 0.84$ fm.

The decomposition into $\widehat{I}$ and $C_{R_E^2}$ and further numerical evaluations of those values are similar to those for the EF term.

The numerical results for eTPE as a function of different values of the separation parameter are summarized in Table II. The minimization of the uncertainty leads to $q_0 \simeq 0.147$ GeV as the optimal value.

The result is

$$I_{\rm eTPE} = \left[-24.14(3.27) + 59.31\, r_p^2\right] \text{ GeV}^{-3} \,, \tag{30}$$

where the error of 2.90 GeV^{-3} corresponds to $\widehat{I}_{\rm eTPE<}$, while the error of 1.53 GeV^{-3} relates to $\widehat{I}_{\rm eTPE>}$.

The individual contributions to the eTPE correction are presented in Table III, while the individual contributions to the uncertainty are summarized in Fig. 9. We see that the individual electric and magnetic recoil contributions are at the level of 10-15%, however, they have a trend for a strong cancellation. The cancellation is rather accidental and depends on the value of the anomalous magnetic moment of the proton κ_p, the mass ratio m/M and the proton radius. The terms differently depend on the parameters and the cancellation of the central values does not produce a massive cancellation of the uncertainties.

However, the latter are much smaller, than the level of the 10% of the Friar-term uncertainty. The size of the contribution is not that important as its sensitivity to the parametrization. It is also important, that any uncertainties at the level of 10% of the Friar-term uncertainty would be important only if it is correlated to the main uncertainty and we have to sum them up linearly rather than as the rms sum. That leaves us with the EF term as the main source of such an uncertainty since it

Contribution	$C_{R_E^2}$ [GeV^{-1}]	$\widehat{I}_{\rm eTPE}$ [GeV^{-3}]	$I_{\rm eTPE}$ [GeV^{-3}]
Fr	2.271	−23.5(3.3)	17.68(3.31)
κ	0	−2.850	−2.850
EF	0.039	1.26(4)	1.97(4)
M1	0	1.76(3)	1.76(3)
M2	−0.0006	−0.838(4)	−0.849(4)
eTPE	2.309	−24.1(3.3)	17.71(3.27)

TABLE III: Individual contributions to the $I_{\rm eTPE}$ at optimal $q_0 \simeq 0.147$ GeV. The last column is for numerical value of $I_{\rm eTPE}$ at $R_E = 0.84$ fm.

is expressed in terms of the same parameters as the leading term. The contribution to the integral by itself can come from a various area of q, however, the area sensitive to the parametrization is around q_0. The expansion at low q ($< q_0$) is the most uncertain at the largest 'low q' available, while the uncertainty of the high-Q area ($> q_0$) is mostly determined by the smallest 'high q' available. The contribution comes from a more broad area than that around $q \sim q_0 \simeq 0.147$ GeV. In the limit $m \ll q_0 \ll M$, the suppression of EF behaves as q_0/M with small coefficients (< 1) as follows from the asymptotic behavior (23). The optimal q_0 is found to be $q_0 \simeq 0.147$ GeV and thus $q_0 < 2m_\mu$. That leads to a suppression of the EF term in respect to the Fr term by a factor of m/M ($\sim 10\%$) with small coefficients (< 1) partly because of additional softening of the integrands by factors $q/2m_\mu < 1$ and softening of the character of the q-integration.

As an important test we check that the scatter due to use of the empiric fits (except for those from [39]) is below the uncertainty. The fits from [39] shift the result somewhat farther, but the value is acceptable because of the unreasonable behavior of the fits at low q.

VI. CONCLUDING REMARKS

The extraction equation is of the similar form as for the Friar term in [12]

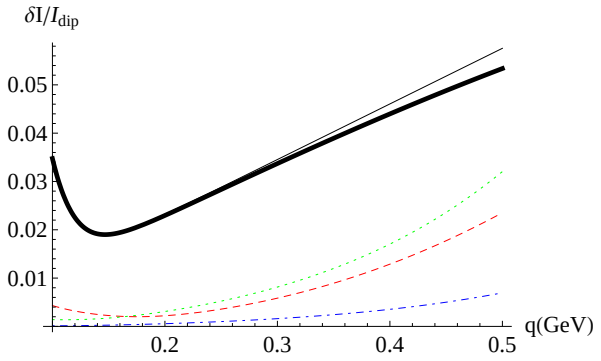


FIG. 9: Individual contributions to the uncertainty $\delta I_{\rm eTPE}$ in relative units of the dipole value for various q_0. The total error δI is presented by the thick solid line, other types of lines are described in the caption of Fig. 4. The recoil contributions are very small and to put all the contributions into the same picture we use different normalization. The values of $\delta I_{\rm eTPE}$ and $\delta I_{\rm Fr}$ are multiplied by 0.1, which allows to use a linear scale (instead of the logarithmic one). The recoil corrections are [anti] correlated with the Friar term, which somewhat reduces the total uncertainty.

Fit	Ref.	Type	$\widehat{I}$ [GeV^{-3}]	$I_{\rm eTPE}$ [GeV^{-3}]
(A1), (A2)	[34]	chain fraction	−24.86	16.99
(A3), (A4)	[34]	chain fraction	−25.01	16.83
(A5), (A6)	[33]	Padé approx. (q^2)	−23.66	18.18
(A7), (A8)	[35]	Padé approx. (q^2)	−24.18	17.66
(A9), (A10)	[36]	Padé approx. (q^2)	−23.86	17.98
(A9), (A11)	[36]	Padé approx. (q^2)	−23.87	17.98
(18), (29)	[37]	Padé approx. (q^2)	−24.14	17.71
(A12), (A13)	[39]	inv. polynom. (q)	−29.31	12.54

TABLE IV: Numerical results for central values of $\widehat{I}$ and $I_{\rm eTPE}$ at the "optimal" $q_0 \simeq 0.147$ GeV from various fits. The last column is for numerical value of $I_{\rm eTPE}$ at $R_E = 0.84$ fm.

$$(R_E)^2 - (R_E^{(0)})^2 = \frac{24(Z\alpha)m_r}{\pi}\frac{1}{1-\frac{24(Z\alpha)m_r}{\pi}C_{R_E^2}(q_0)}\left[C_{R_E^2}(q_0)(R_E^{(0)})^2 + \left(\widehat{I}_{\rm eTPE}(q_0) - I^0_{\rm eTPE}(q_0)\right)\right], \qquad (31)$$

where $I^0_{\rm eTPE}$ is the original result for $I_{\rm eTPE}$ and $\widehat{I}_{\rm eTPE}$ is the one from which we removed the R_E^2 term. The coefficient $C_{R_E^2}$ is due to a small 'renormalization' of the R_E^2 term.

In the case of the Friar term the 'renormalization' is

$$1 \to 1 - \frac{8(Z\alpha)}{\pi}\frac{m_r}{q_0}$$

and the recoil effects weakly affect it. For $I^0_{\rm eTPE}$ we use here the result from [13] with the F_1^2 term restored as suggested in [14]

$$\begin{aligned} I^0_{\rm eTPE} &= \Big(27.5(1.6) - 4.5\Big)\ {\rm GeV}^{-3} \\ &= 23.0(1.6)\ {\rm GeV}^{-3}\,. \end{aligned} \qquad (32)$$

That is related to the evaluation in [1].

Eventually, we arrive at

$$R_E = 0.840\,22(53)\ {\rm fm}\,, \qquad (33)$$

which is to be compared with the original result $R_E =$

0.840 87(39) fm from [1] (which we use here as the reference value $R_E^{(0)}$) and the result $R_E = 0.840\,22(56)$ fm corrected for the self-consistent evaluation of the Friar term [12]. Note that in both papers on the self-consistent reevaluation ([12] and this paper) only a correction was found, while all the other theory remains the same as used in [1].

Various extractions of the proton charge radius are summarized in Table V. The main effect of the self-consistent evaluation comes from the correction for the Friar term. The results of [12] and this paper, while correcting the Friar term, have a marginal difference which confirms that the assumption, that while calculating the G^2 term of $I_>$ a small area of the data around the low limit dominates, is valid. The result of the complete evaluation is marginally different from the result of the re-evaluation of the Friar term only. The strong cancellation between corrections from various contributions is rather accidental, while the marginal shift of the uncertainty is rather expected, because the corrections to $I_{\rm eTPE}$ are small and less sensitive.

R_E [fm]	$I_{\rm eTPE}$ [GeV^{-3}]	Comments
0.840 87(39)	23.0(1.6)	R_E from [1], $I_{\rm eTPE}$ from [14]
0.840 22(56)	17.7(3.4)	$I_{\rm Fr}$ from [12], $I_{\rm rec}$ from [14]
0.840 21(53)	17.7(3.3)	$I_{\rm Fr}$ from this work, $I_{\rm rec}$ from [14]
0.840 22(53)	17.7(3.3)	$I_{\rm eTPE}$ from this work

TABLE V: The results of various evaluations of the proton charge radius. The theory follows [1] except of the treatment of the eTPE term. The eTPE term in [1] was found following [14]. The result from [12] dealt with the correction of the Friar term only. The recoil part of the eTPE is added to the Fr contributions accordingly to [13, 14]. One of the result of *this paper* was obtained also by correcting the Fr term only, while the other is a result of the complete results of the self-consistent evaluation here.

The uncertainty of the result (33) comes from our knowledge of the curvature of $G_E(q^2)$ at low q and on our accuracy of the data on G_E around $q = 0.1 - 0.2$ GeV. Any improvement of those will immediately improve accuracy of determination of the proton charge radius from muonic hydrogen.

Acknowledgments

The authors are grateful to Jose Manuel Alarcón, Igor Anikin, John Arrington, Jan Bernauer, Michael Birse, Vladimir Braun, Carl Carlson, Victor Chernyak, Michael Distler, Dieter Drechsel, Simon Eidelman, Ron Gilman, Misha Gorshteyn, Richard Hill, Vadim Lensky, Ina Lorenz, Judith McGovern, Ulf Meissner, Vladimir Pascalutsa, Gil Paz, Randolf Pohl, Guy Ron, Akaki Rusetsky, Ingo Sick, and Marc Vanderhaeghen for stimulating and useful discussions. The work was supported in part by DFG (under grant # HA 1457/9-1) and by RFBR (under grant # 14-02-91332).

Appendix A: Fits for the electric and magnetic form factors of the proton applied in the paper

The results in the paper have been obtained by evaluation with the fits from [37]. However, it is important to be sure that the result does not depend on details of the fits and in particular on details of their expansion around $q = 0$ and their asymptotics at high q. Various fits for G_E and G_M are applied in this paper for test purposes.

The fits include two pairs of the chain-fraction fits. Both are from Arrington and Sick, 2007, [34]. The first one is completely based on [34]

$$G_E(q^2) = \frac{1}{1+\frac{3.44Q^2}{1-\frac{0.178Q^2}{1-\frac{1.212Q^2}{1+\frac{1.176Q^2}{1-0.284Q^2}}}}} \qquad \text{(A1)}$$

and

$$\frac{G_M(Q^2)}{\mu_p} = \frac{1}{1+\frac{3.173Q^2}{1-\frac{0.314Q^2}{1-\frac{1.165Q^2}{1+5.619\frac{Q^2}{1-1.087Q^2}}}}}\,, \qquad \text{(A2)}$$

where, Q is the numerical value for the momentum transfer q in GeV.

The other pair is obtained in [34] by applying the two-photon correction according to [41]

$$G_E(q^2) = \frac{1}{1+\frac{3.478Q^2}{1-\frac{0.140Q^2}{1-\frac{1.311Q^2}{1+\frac{1.128Q^2}{1-0.233Q^2}}}}} \qquad \text{(A3)}$$

and

$$\frac{G_M(q^2)}{\mu_p} = \frac{1}{1+\frac{3.224Q^2}{1-\frac{0.313Q^2}{1-\frac{0.868Q^2}{1+\frac{4.278Q^2}{1-1.102Q^2}}}}}\,. \qquad \text{(A4)}$$

Other fits are with the Padé approximation in q^2, originally introduced by Kelly, 2004, such as [33]

$$G_E = \frac{1-0.24\tau_p}{1+10.98\tau_p+12.82\tau_p^2+0.863\tau_p^3} \qquad \text{(A5)}$$

and

$$\frac{G_M(q^2)}{\mu_p} = \frac{1+0.12\tau_p}{1+10.97\tau_p+18.86\tau_p^2+6.55\tau_p^3}\,. \qquad \text{(A6)}$$

The Padé approximations have been later developed by Arrington et al., 2007, [35]

$$G_E - \frac{1 + 3.439\tau_p - 1.602\tau_p^2 + 0.068\tau_p^3}{1 + 15.055\tau_p + 48.061\tau_p^2 + 99.304\tau_p^3 + 0.012\tau_p^4 + 8.650\tau_p^5} \tag{A7}$$

and

$$\frac{G_M(q^2)}{\mu_p} = \frac{1 - 1.465\tau_p + 1.260\tau_p^2 + 0.262\tau_p^3}{1 + 9.627\tau_p + 11.179\tau_p^4 + 13.245\tau_p^5} \tag{A8}$$

In paper [36] by Alberico et al., 2009, one electric fit is presented

$$G_E(q^2) = \frac{1 - 0.19\tau_p}{1 + 11.12\tau_p + 15.16\tau_p^2 + 21.25\tau_p^3} \tag{A9}$$

and two magnetic ones

$$\frac{G_M(q^2)}{\mu_p} = \frac{1 + 1.53\tau_p}{1 + 12.87\tau_p + 29.16\tau_p^2 + 41.40\tau_p^3} \tag{A10}$$

$$\frac{G_M(q^2)}{\mu_p} = \frac{1 + 1.09\tau_p}{1 + 12.31\tau_p + 25.57\tau_p^2 + 30.61\tau_p^3} \tag{A11}$$

The most recent Padé-approximation fits (see (18) and (29)) are presented by and Venkat et al., 2011, [37] and have been used in the main body of the paper for all the evaluations.

One more pair of the fits with is with the inverse polynomials in q from Bosted, 1995, [39]

$$G_E(q^2) = \frac{1}{1 + 0.62Q + 0.68Q^2 + 2.8Q^3 + 0.83Q^4} \tag{A12}$$

and

$$\frac{G_M(q^2)}{\mu_p} = \left(1 + 0.35Q + 2.44Q^2 + 0.50Q^3 + 1.04Q^4 + 0.34Q^5\right)^{-1} . \tag{A13}$$

That is a phenomenological fit designed to be used for medium and high q. It is not expected to be appropriate at low q. Providing a reasonably good approximation at medium momentum transfer, the fit apparently has incorrect low-q behavior and incorrect analytic properties such as a branch point at $q^2 = 0$.

[1] A. Antognini, F. Nez, K. Schuhmann, F.D. Amaro, F. Biraben, J.M.R. Cardoso, D.S. Covita, A. Dax, S. Dhawan, M. Diepold, L.M.P. Fernandes, A. Giesen, A.L. Gouvea, T. Graf, T.W. Hänsch, P. Indelicato, L. Julien, Cheng-Yang Kao, P. Knowles, F. Kottmann, E.-O. Le Bigot, Yi-Wei Liu, J.A.M. Lopes, L. Ludhova, C.M.B. Monteiro, F. Mulhauser, T. Nebel, P. Rabinowitz, J.M.F. dos Santos, L.A. Schaller, C. Schwob, D. Taqqu, J.F.C. A. Veloso, J. Vogelsang, R. Pohl, Science, **339** 417 (2013).

[2] M.I. Eides, H. Grotch, and V.A. Shelyuto, *Theory of Light Hydrogenic Bound States* (Springer, Berlin-Heidelberg-New York, 2007).

[3] U. D. Jentschura, Ann. Phys. **326**, 500 (2011).

[4] P.J. Mohr, B.N. Taylor, and D.B. Newell, Rev. Mod. Phys. **84**, 1527 (2012).

[5] J.C. Bernauer, P. Achenbach, C. Ayerbe Gayoso, R. Böhm, D. Bosnar, L. Debenjak, M.O. Distler, L. Doria, A. Esser, H. Fonvieille, J.M. Friedrich, J. Friedrich, M. Gómez Rodríguez de la Paz, M. Makek, H. Merkel, D.G. Middleton, U. Müller, L. Nungesser, J. Pochodzalla, M. Potokar, S. Sánchez Majos, B.S. Schlimme, S. Širca, Th. Walcher, and M. Weinriefer, Phys. Rev. Lett. **105**, 242001 (2010).

[6] I. Sick, Phys. Lett. B **576**, 62 (2003); Can. J. Phys. **85**, 409 (2007).

[7] X. Zhan, K. Allada, D.S. Armstrong, et al., Phys. Lett. B **705**, 59 (2011).

[8] I. Sick and D. Trautmann, Phys. Rev. C **89**, 012201 (2014).

[9] S.G. Karshenboim, Phys. Lett. A**225**, 97 (1997).

[10] M.O. Distler, J.C. Bernauer, and Th. Walcher, Phys. Lett. B**696**, 343 (2011).

[11] S.G. Karshenboim, Annalen der Physik **525**, 472 (2013); Phys. Usp. **56**, 883 (2013).

[12] S.G. Karshenboim, Phys. Rev. D **90**, 053012 (2014).

[13] C.E. Carlson and M. Vanderhaeghen, Phys. Rev. A**84**, 020102 (2011).

[14] M.C. Birse and J.A. McGovern, Eur. Phys. J. A**48**, 120 (2012).

[15] J. L. Friar, Phys. Lett. **80**B, 157 (1979).

[16] J. L. Friar, Ann. Phys. (NY) **122**, 151 (1979).

[17] L. A. Borisoglebsky and E. E. Trofimenko, Phys. Lett. **81**B, 175 (1979).

[18] K. Pachucki, Phys. Rev. A **53**, 2092 (1996).

[19] G.P. Lepage. Phys. Rev. A**16**, 863 (1977);
G.T. Bodwin, D.R. Yennie and M.A. Gregorio. Rev. Mod. Phys. **57**, 723 (1985);
M.I. Eides, S.G. Karshenboim and V.A. Shelyuto, Ann. Physics **205**, 231 (1991).

[20] J. Sapirstein and D.R. Yennie, In T. Kinoshita (Ed.), *Quantum Electrodynamics* (World Sci., Singapore, 1990), pp. 560–672.

[21] K. Pachucki, Phys. Rev. A 60, 3593 (1999).

[22] A.P. Martynenko and R.N. Faustov, Yad. Phys. **63**, 915

(2000); Phys. Atom. Nuclei **63**, 845 (2000).
[23] A. P. Martynenko, Yad. Phys. **69**, 1344 (2006); Phys. At. Nucl. **69**, 1309 (2006).
[24] D. Nevado and A. Pineda, Phys. Rev. C **77**, 035202 (2008).
[25] J.M. Alarcón, V. Lensky, and V. Pascalutsa, Eur. Phys. J. C**74**, 2852 (2014).
[26] C. Peset and A. Pineda, Nucl. Phys. B **887**, 69 (2014).
[27] M. Gorchtein, F.J. Llanes-Estrada, and A.P. Szczepaniak, Phys. Rev. A **87**, 052501 (2013).
[28] S.G. Karshenboim, Phys. Rev. D **90**, 053013 (2014).
[29] J. Arrington, Phys. Rev. Lett. **107**, 119101 (2011).
[30] J.C. Bernauer, P. Achenbach, C. Ayerbe Gayoso, R. Böhm, D. Bosnar, L. Debenjak, M.O. Distler, L. Doria, A. Esser, H. Fonvieille, J.M. Friedrich, J. Friedrich, M. Gómez Rodríguez de la Paz, M. Makek, H. Merkel, D.G. Middleton, U. Müller, L. Nungesser, J.Pochodzalla, M.Potokar, S. Sánchez Majos, B.S. Schlimme, S. Širca, Th. Walcher, and M. Weinriefer, Phys. Rev. Lett. **107**, 119102 (2011).
[31] I. Sick, Prog. Part. Nucl. Phys. **67**, 473 (2012).
[32] F. Jegerlehner, *The Anomalous Magnetic Moment of the Muon*. Springer, Berlin and Heidelberg: Springer Tracts in Modern Physics **226** (2007).
[33] J.J. Kelly, Phys. Rev. C **70**, 068202 (2004).
[34] J. Arrington and I. Sick, Phys. Rev. C**76**, 035201 (2007).
[35] J. Arrington, W. Melnitchouk, and J.A. Tjon, Phys. Rev. C**76**, 035205 (2007).
[36] W.M. Alberico, S.M. Bilenky, C. Guinti, and K.M. Graczyk, Phys. Rev. C**79**, 065204 (2009).
[37] S. Venkat, J. Arrington, G.A. Miller and X. Zhan, Phys. Rev. C**83**, 015203 (2011).
[38] J. Bernauer, *Measurement of the elastic electron-proton cross section and separation of the electric and magnetic form factor in the Q^2 range from 0.004 to 1* $(\mathrm{GeV}/c)^2$. Ph.D. Thesis, Mainz, 2010. Available at http://wwwa1.kph.uni-mainz.de/A1/publications/doctor/bernauer.p
[39] P.E. Bosted, Phys. Rev. C**51**, 409 (1995).
[40] J.L. Friar and I. Sick, Phys. Rev. A**72**, 040502 (2005).
[41] P.G. Blunden, W. Melnitchouk, and J.A. Tjon, Phys. Rev. C**72**, 034612 (2005).